

Magnetic properties of dredged oceanic gabbros and the source of marine magnetic anomalies

D. V. Kent *Lamont-Doherty Geological Observatory, Columbia University,* Palisades, New York 10964, USA*

B. M. Honnorez *Rosenstiel School of Marine and Atmospheric Science, University of Miami, Miami, Florida 33149, USA*

N. D. Opdyke* *Department of Geological Sciences, Columbia University, New York, New York 10027, USA*

P. J. Fox* *Department of Geological Sciences, State University, Albany, New York 12222, USA*

Received 1978 May 10; in original form 1978 January 16

Summary. Magnetic property studies (natural remanent magnetization, initial susceptibility, progressive alternating field demagnetization and magnetic mineralogy of selected samples) were completed on 45 samples of gabbro and metagabbro recovered from 14 North Atlantic ocean-floor localities. The samples are medium to coarse-grained gabbro and metagabbro which exhibit subophitic intergranular to hypidiomorphic granular igneous textures. The igneous mineralogy is characterized by abundant plagioclase, varying amounts of clinopyroxene and hornblende, and lesser amounts of magnetite, ilmenite and sphene. Metamorphic minerals (actinolite, chlorite, epidote and fine-grained alteration products) occur in varying amounts as replacement products or vein material. The opaque mineralogy is dominated by magnetite and ilmenite. The magnetite typically exhibits a trellis of exsolution-oxidation ilmenite lamellae that appears to have formed during deuteric alteration.

The NRM intensities of the gabbros range over three orders of magnitude and give a geometric mean of 2.8×10^{-4} gauss and an arithmetic mean of 8.8×10^{-4} gauss. The Königsberger ratio, a measure of the relative importance of remanent to induce magnetization, is greater than unity for the majority of the samples and indicates that remanent magnetization on average dominates the total magnetization of oceanic gabbros in the Earth's magnetic field. The magnetic properties of fresh and metamorphosed gabbros appeared to be similar. The majority of gabbros studied were characterized by median destructive fields greater than 200 Oe. The high stability is attributed largely to the effective subdivision of the magnetite grains by the

* Also: Lamont-Doherty Geological Observatory, Columbia University, Palisades, New York 10964, USA.

ilmenite lamellae. Model studies based on a magnetization distribution in the oceanic crust inferred from the magnetic property analysis of representative rock bodies within the oceanic crust, suggest that remanent magnetic contrasts in the gabbroic rocks of Layer 3 can be expected to contribute significantly to the generation of sea-floor spreading-type marine magnetic anomalies.

1 Introduction

As originally conceived by Vine & Matthews (1963), lineated marine magnetic anomalies arise from magnetization contrasts between normally- and reversely-magnetized oceanic crust. Although not a critical factor in their hypothesis, it was assumed that the vertical extent of the magnetic crust was defined by the depth to the Curie point isotherm, on the order of 20 km below sea-level and well into the upper mantle. Subsequently, Vine & Wilson (1965) considered that the bulk of the remanent magnetization resides in a comparatively thin (1 or 2 km thick) layer of basalts which overlies a main crustal layer of serpentinite that is weakly magnetized; this proposition was based on magnetic properties inferred for a petrologic model of the ocean crust after Hess (1965). The level of the magnetic source layer was further constrained to lie just in the upper part (Layer 2A) of basaltic Layer 2 by deducing the bulk magnetization of topographic features from the associated short-wavelength magnetic anomalies (Talwani, Windisch & Langseth 1971; Atwater & Mudie 1973). Assuming a constant uniform magnetization intensity of $5\text{--}15 \times 10^{-3}$ gauss for Layer 2A, a source layer thickness of about 0.5 km appears to be consistent with the observed magnetic anomalies on several ridge systems (e.g. Klitgord *et al.* 1975).

Measurements of the magnetic properties of dredged and drilled (Deep Sea Drilling Project) oceanic basalts generally give only partial support to the concept of a thin magnetic source layer. This data has been summarized recently by Lowrie (1977). The evidence from oceanic surveys and from dredged basalts concur for very high axial zone Layer 2A magnetizations, averaging in the range $20\text{--}50 \times 10^{-3}$ gauss. However, over the ridge flanks the inferred magnetization from magnetic surveys appears to be a factor of two greater than the measured values for DSDP basalts. If the average remanent magnetization value obtained from DSDP basalts is assumed to be representative of the magnetic source layer, then its thickness must exceed a kilometre to account for magnetic anomaly amplitudes (Lowrie 1974, 1977; see also Johnson & Atwater 1977; Ryall *et al.* 1977). Alternatively, a significant fraction of anomaly amplitudes may originate from an additional magnetic source deeper in the oceanic crust, perhaps in Layer 3.

In contrast to oceanic basalts, the magnetic properties of rocks representative of deeper levels in the oceanic crust are less well known simply because fewer samples are available. It is often supposed that the coarse-grained intrusive rocks in the lower crust are weakly magnetized, with low remanent stabilities and Königsberger ratios. For this reason, the magnetic source layer is usually thought to be essentially confined to the demonstrably highly magnetized basalts which comprise the extrusive and shallow intrusive rocks of Layer 2. However, the large volume of material available below the second layer of the oceanic crust may compensate at least in part for the weaker magnetizations that may characterize these rocks and therefore these deeper seated rocks may make a significant contribution to the observed magnetic anomalies. The magnitude and nature of the effect would depend on the characteristics and origin of the remanent magnetizations.

We attempt here to characterize the magnetic properties of a suite of oceanic gabbros that may be representative of deeper levels in the oceanic crust, particularly Layer 3.

Table 1. Positions, depths and morphologic provinces of dredged samples selected for measurement of magnetic properties.

Dredge station	Location	Depth (m)	Morphologic province
(1) V30-D1	1° 01' N 25° 06' W	3347	St Paul F.Z.
(2) V30-D5	1° 31' N 19° 06' W	~5571	St Paul F.Z.
(3) V30-D12	35° 04' N 35° 09' W	2675–2550	Oceanographer F.Z.
(4) V30-D18	35° 04' N 35° 29' W	3250–3175	Oceanographer F.Z.
(5) V30-D19	35° 05' N 35° 29' W	3293–2926	Oceanographer F.Z.
(6) V30-D20	35° 04' N 35° 28' W	3250–3175	Oceanographer F.Z.
(7) AT 5M (A–B–C)	1° 07' S 14° 52' W	5370–5170	Chain F.Z. *
(8) AT 11A	0° 18' N 17° 14' W	5305–5100	Romanche F.Z.
(9) AT 25F	0° 22' S 20° 09' W	5300–5100	Romanche F.Z.
(10) AT 155M	0° 14' S 18° 09' W	7316–5950	Romanche F.Z.
(11) AT 77J-L	10° 56' N 43° 36' W	3850–4900	Vema F.Z.
(12) AT 79 (AA–BB)	10° 46' N 42° 48' W	4150–5200	Vema F.Z.

Forty-five samples of gabbro and metagabbro, taken from 14 dredge hauls on tectonic escarpments in the Atlantic Ocean (Table 1), were selected for study. One to three cylindrical (2.5 cm diameter × 2.2 cm high) specimens were taken from up to six samples from each dredge. The natural remanent magnetization (NRM) and the initial susceptibility (k) of each specimen were measured with a 105^oHz spinner magnetometer and an AC bridge, respectively. One specimen from each sample was subjected to progressive alternating field (AF) demagnetization to characterize the stability of magnetization. The magnetic mineralogy of selected samples was investigated by Curie temperature analysis and reflected-light microscopy.

2 Petrography of the gabbros

2.1 SILICATE MINERALOGY

The 45 gabbroic samples chosen for magnetic property analysis exhibit characteristics typical of plutonic rocks recovered from the ocean-floor escarpments. The samples range from medium- to coarse-grained and exhibit subophitic, intergranular or hypidiomorphic-granular igneous textures. The gabbros are characterized by a wide range of primary silicate mineralogy and many samples have experienced varying degrees of low-temperature alteration (Table 2). The 22 samples from the Oceanographer Fracture Zone are composed of abundant (> 30 per cent) calcic plagioclase with lesser and variable amounts (10–30 per cent) of clinopyroxenes, brown hornblende and green hornblende; opaque minerals, sphene and apatite occur as minor (< 10 per cent) phases. The Oceanographer Fracture Zone gabbros reflect the complete spectrum of greenschist facies low-temperature alteration. Several samples have only been incipiently altered and have minor veinlets of chlorite and/or actinolite anastomosing through the sample. More pervasively altered gabbros are characterized by varying amounts, and any combination, of the following minerals: actinolite, chlorite, epidote, white mica and blue-green hornblende. These low-temperature alteration minerals rim or replace primary silicate phases as well as occur in veins and veinlets. Fine-grained opaque blebs were observed in a few samples to be in association with actinolite or chlorite. Retrograde low-temperature alteration was suggested in several samples by the occurrence of zeolite minerals.

Table 2. Measured magnetic properties of 45 dredged oceanic gabbro samples.

Dredge	Sample	Rock type	NRM (10^{-4} G)	K (10^{-4} G/Oe)	Q_n	MDF (Oe)
V30-D1	1	Hornblende–augite gabbro	1.71	0.82	7.3	>400
	2	Olivine–augite gabbro	5.19	8.20	2.2	85
	3	Olivine–augite gabbro	2.32	0.64	12.7	>400
	4	Olivine–augite gabbro	0.73	1.42	1.8	185
	5	Hornblende–augite gabbro	2.18	0.76	10.1	>400
V30-D5	1	Hornblende–augite gabbro	0.81	0.40	7.1	250
	2	Metamorphosed hornblende–augite gabbro	3.19	0.49	14.8	>400
	3	Metamorphosed gabbro	0.26	0.43	2.1	>400
	4	Metamorphosed gabbro	0.10	0.50	0.7	>400
	5	Metamorphosed gabbro	0.69	0.40	6.0	>400
	6	Metamorphosed gabbro	0.11	0.30	1.3	>400
	7	Metamorphosed gabbro	0.77	0.62	4.4	>400
V30-D12	P4	Metamorphosed gabbro	11.6	123.6	0.2	75
	P7	Metamorphosed hornblende gabbro	11.6	74.4	0.4	25
	P14	Metamorphosed gabbro	19.4	88.3	0.5	25
V30-D18	P1	Metamorphosed hornblende gabbro	0.14	0.97	0.3	300
	P2	Metamorphosed hornblende gabbro	79.8	145.2	1.3	150
	P13	Metamorphosed gabbro	2.35	0.94	5.7	300
	P15	Metamorphosed hornblende gabbro	0.15	1.11	0.3	300
	P17	Metamorphosed hornblende gabbro	2.57	0.85	6.9	>400
	P19	Metamorphosed hornblende gabbro	18.2	64.7	0.6	25
	P22	Metamorphosed hornblende gabbro	0.59	1.45	0.9	>400
	P28	Metamorphosed gabbro	14.5	45.0	0.7	75
	P30	Metamorphosed hornblende gabbro	13.1	38.5	0.8	150
V30-D19	P5	Metamorphosed gabbro	1.65	1.28	2.9	>400
	P11	Metamorphosed gabbro	26.0	59.3	1.0	>400
	P12	Metamorphosed hornblende gabbro	4.35	0.71	13.9	>400
V30-D20	P1	Metamorphosed hornblende gabbro	0.40	0.59	1.6	>400
	P2	Metamorphosed hornblende gabbro	0.52	0.94	1.3	>400
	P4	Metamorphosed gabbro	5.86	7.33	1.8	>400
	P5B	Metamorphosed hornblende gabbro	26.7	0.65	92.9	>400
	P6	Metamorphosed gabbro	0.28	0.48	1.3	>400
	P7	Metamorphosed hornblende gabbro	6.54	0.74	20.3	>400
	P14	Metamorphosed gabbro	5.91	0.57	23.5	>400
	AT5	MA	Noritic gabbro	6.86	8.38	2.9
AT11	A	Metamorphosed gabbro	6.50	29.3	0.8	>400
AT25	F	Alkali gabbro	3.09	5.88	1.85	125
AT77	J	Noritic gabbro	17.8	72.9	0.7	75
	L	Noritic gabbro	314.4	68.1	13.6	25
	S	Noritic gabbro	40.2	120.7	1.0	125
AT79	AA	Noritic gabbro	21.0	93.1	0.7	150
	BB	Gabbro	4.13	6.37	1.9	200
	CC	Noritic gabbro	3.26	2.51	3.82	300
AT155	M	Troctolitic gabbro	2.33	11.3	0.7	300
	P	Troctolitic gabbro	15.9	11.6	4.8	300

Twelve gabbros recovered in dredges located along escarpments of the St Paul's Fracture Zone are either hornblende-augite gabbro characterized by abundant plagioclase, clinopyroxene and lesser hornblende, or olivine-augite gabbro composed of plagioclase and augite with subordinate olivine. Opaque grains occur in minor amounts in all samples and minor amounts of talc, serpentine and smectite are associated with olivine in the olivine-bearing gabbros. Veinlets of chlorite and/or actinolite are observed in a few samples and several gabbros have been intensely altered with blue-green hornblende and chlorite occurring in abundance.

The majority of the gabbro samples from the Vema, Romanche and Chain Fracture zones dredge collections are noritic gabbros composed of calcic plagioclase, hypersthene and salite; apatite and opaque phases occur as accessory primary minerals. The collection also included a troctolitic gabbro (plagioclase, fosterite and bronzite), a gabbro (plagioclase and augite with accessory opaque phases) and an alkali gabbro (plagioclase, titanogaugite with accessory analcite nepheline, chrome spinel and opaque phases). All these gabbro samples from the Vema, Romanche and Chain Fracture Zones have experienced low-temperature alteration and the following associations have been observed: actinolite and hornblende after pyroxene; albite and smectite after plagioclase; opaque phases alter to maghemite, Fe-hydroxides and hematite; iddingsite, talc and magnetite after olivine; smectite, chlorite and zeolites (analcite, chabazite and gonnardite) occur in veins and veinlets. One greenschist facies metagabbro was sampled and was characterized by relict primary plagioclase and clinopyroxene and abundant secondary actinolite, hornblende, albite, chlorite, smectite, analcite, hematite, maghemite and rutile.

2.2 MAGNETIC MINERALOGY

Curie-point analysis and microscopic examination of polished sections were used to characterize the magnetic mineralogy of selected gabbro samples. For Curie-point determinations, small chips from a gabbro sample were ground to a coarse powder and heated in air from room temperature to about 680°C in the presence of an applied field of 4000 Oe, using a vertical-motion type Curie balance. The variation of saturation magnetization with temperature was recorded continuously on an *X-Y* recorder. Temperature calibration was accurate to within 5°C; magnetization measurements were uncalibrated. Uninterpretable thermomagnetic curves were obtained for about one-quarter of the samples analysed due to an apparently insufficient concentration of magnetic mineral.

The thermomagnetic curves of most of the remaining samples were fairly uniform in appearance and of the types illustrated in Fig. 1(a), (b), (c). The thermomagnetic behaviour was essentially reversible with heating and cooling, and showed a single well-defined Curie point. Although most samples gave block-shaped thermomagnetic curves (Fig. 1(a) and (b)) several samples showed a more rapid initial decrease in magnetization (Fig. 1(c)) which can be attributed to the presence of an appreciable fraction of a paramagnetic mineral. A paramagnetic contribution to the total magnetization of this sample is also indicated by the relatively large value of magnetization remaining after the Curie point of the dominant ferromagnetic constituent has been exceeded (Fig. 1(c)).

The characteristic Curie temperature was determined from the heating curve of each sample using the graphical method of Grommé, Wright & Peck (1969); the distribution of Curie temperatures in the gabbro samples is shown in Fig. 2. Except for two samples which gave Curie points of 680 and 270°C, respectively, the Curie points fall in the range 550 to 590°C, with a prominent grouping about the mean value of 575°C. These Curie temperatures are indicative of magnetite as the dominant magnetic mineral in the samples.

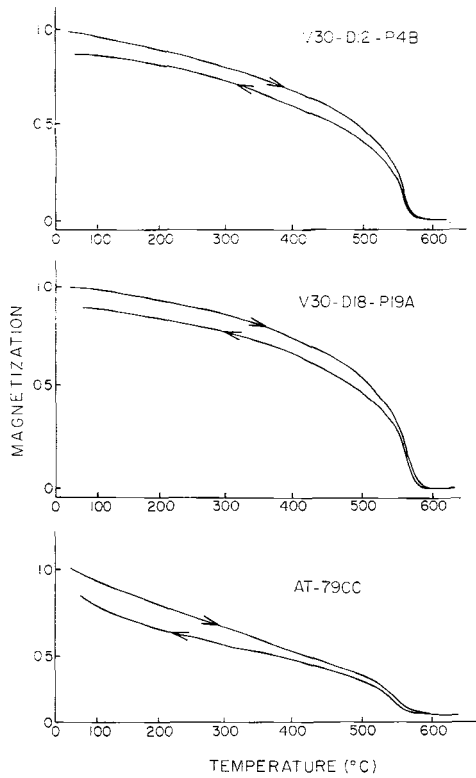


Figure 1. Representative high-field (4 kOe) thermomagnetic curves for dredged oceanic gabbros. Heating and cooling in air; magnetization in arbitrary units. Note difference in plotted position of base line (i.e. magnetization zero) for each curve.

The sample (AT-11A) with the higher initial Curie point of 680°C gave an irreversible thermomagnetic curve (Fig. 3(a)); the Curie point on the cooling portion of the curve was 510°C and there was a substantial increase in magnetization after thermal cycling. (Note also the large change in magnetization in the low-temperature range during both heating and cooling which may again be indicative of a sizeable paramagnetic fraction.) The Curie

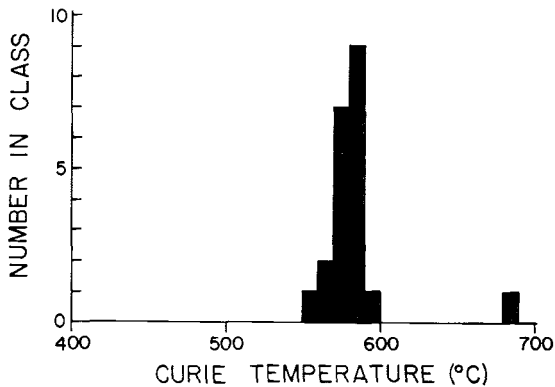


Figure 2. Frequency distribution of Curie temperatures determined from heating cycle of high-field thermomagnetic curves of 22 dredged oceanic gabbro samples (sample AT 25F with Curie point of 270°C not plotted).

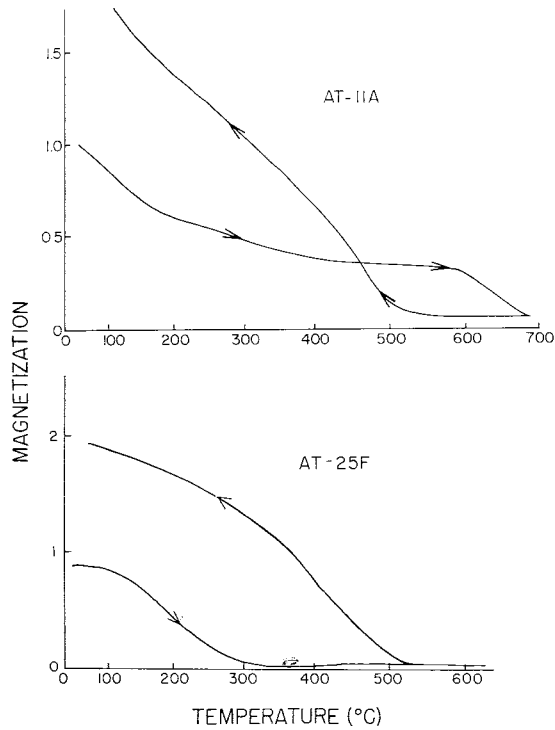


Figure 3. High-field thermomagnetic curves for dredged oceanic gabbro samples AT-11A (top) and AT-25F (bottom). Heating and cooling in air; magnetization in arbitrary units.

temperature of 680°C is near to that of hematite. However, the nature of the chemical alteration during thermal cycling in air which can result in the production of a more highly magnetic mineral with a lower Curie temperature, at the apparent expense of the hematite, is not clear but might imply reducing conditions on a local scale in the sample.

The sample (AT-25F), with the low initial Curie point of 270°C, also gave an irreversible thermomagnetic curve with a substantial increase in magnetization but with an increased Curie point (to 520°C) after thermal cycling (Fig. 3(b)). This thermomagnetic behaviour can be accounted for by the initial presence of a titanomagnetite or titanomaghemite which separates upon heating to a titanium-rich phase (hemo-ilmenite) and a titanium-poor phase near to magnetite in composition. On cooling from high temperature the stronger magnetization of this magnetite appears at a high Curie temperature and increases to its room temperature value.

Examination of polished sections of representative gabbro samples by reflected-light and transmitted-light microscopy provides good support for the inferences drawn from the thermomagnetic characteristics as well as giving an indication of the origin of the opaque mineralogy. The opaque minerals generally constitute about 10 per cent of the gabbro samples and appear to be interstitial with the primary igneous silicate phases (e.g. plagioclase, clinopyroxene), but were also found associated with metamorphic assemblages (e.g. actinolite, blue-green amphibole) in some samples. The opaque minerals identified are most commonly magnetite and ilmenite assemblages, the estimated ratio of magnetite to ilmenite in the range 1:35 to occasionally 1:1. The presence of magnetite as the dominant magnetic mineral in the gabbro samples is therefore indicated by both sets of observations, thermomagnetic and microscopic, whereas the paramagnetic behaviour evident in some of

the thermomagnetic curves (e.g. Fig. 1(c)) can be attributed to the observed high abundance of ilmenite which has a Curie point below room temperature.

Grains of ilmenite usually appear homogeneous even under 1200× magnification. On the other hand, the larger magnetite grains are almost always characterized by a trellis pattern of ilmenite lamellae, usually of two generations and arranged along the [111] planes of the magnetite host (Plate 1a). In addition, very fine rods of exsolved spinel may be found along the [100] planes of magnetite (Plate 1b). In some samples, the ilmenite lamellae have been altered to sphene and rutile while martite is seen to have partially replaced magnetite. Magnetite also occurs sporadically in a few specimens as fine grains and along cleavages in pyroxene; this, however, may be a primary igneous association. In a few samples (e.g. AT155) magnetite is clearly secondary as it occurs in cracks and around serpentinized olivine grains and may have formed long after the initial cooling of the rock (Watkins & Haggerty 1967). For most of the samples examined, however, the opaque mineralogical characteristics are indicative of advanced oxidation which most likely occurred during *deuteric alteration* (Haggerty 1976).

Two samples had quite different opaque mineralogies compared to the other gabbros examined and are those with the anomalous thermomagnetic behaviours. Sample AT-11A, a greenschist facies metagabbro, had ilmenite grains containing abundant 'thin' bodies of magnetite, oriented parallel to the (001) planes of the host. Some magnetite rodlets are partially pseudomorphed by a grey-blue coloured phase (maghemite?) and others by hematite (or titanohematite). Toward the edges of the ilmenite grains the rods of magnetite have been oxidized to hematite and patches of a complex mineral assemblage of rutile and titanohematite have also developed (Plate 1c). The coexisting grains of magnetite contain abundant oxidation-exsolution ilmenite lamellae forming a trellis pattern and scarce exsolved rods of spinel oriented in the [100] planes. Martitization of magnetite is quite common. These opaque mineralogical characteristics are comparable to assemblages in metasomatic rocks described by Buddington, Fahey & Vlisidis (1963), Buddington & Lindsley (1964) and Haggerty (1976) and imply several stages of alteration under different conditions of temperature and oxygen fugacity. The common occurrence of hematite in this sample, both in magnetite grains (as martite) and in ilmenite grains (as hematite in rodlets and fine aggregate with rutile), is also indicated by Curie temperature analysis which showed a high Curie point (Fig. 3(a)). Although martite was sometimes observed in a microscopic examination of other samples, a thermomagnetic expression was not apparent, presumably due to small amounts of the more weakly magnetic hematite in the presence of magnetite which was dominant volumetrically and magnetically in most of the other samples.

Another sample (AT-25F), an alkali gabbro, is completely different from the rest of the gabbros in that it has large skeletal, homogeneous titanomagnetites, elongated skeletons of ilmenite and early crystallized small rounded chrome-spinel (Plate 1d). Moreover, the titanomagnetite has very abundant volume-change cracks along which a fine-grained greyish-blue coloured phase has started to replace the host from the edges toward the core of the grain, which mostly remained unaltered. The Curie temperature analysis of this sample, as discussed earlier, is in accord with the observed magnetic mineralogy which reflects a low oxidation state more typically found in oceanic basalts (Ozima & Ozima 1971; Lowrie 1974).

3 Magnetic properties

3.1 NRM INTENSITIES AND KONIGSBERGER RATIOS

In contrast to the relatively uniform magnetic mineralogy, as indicated by the thermomagnetic and microscopic observations, the magnetizations of the oceanic gabbro samples

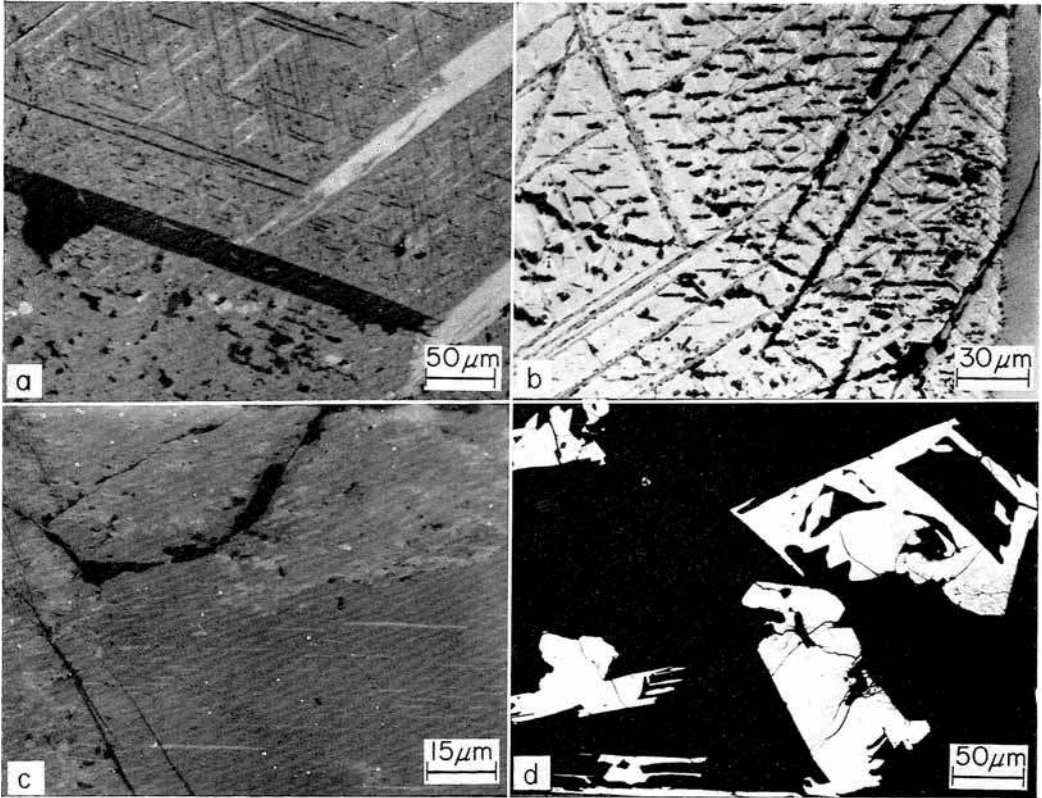


Plate 1. Photomicrographs in reflected light of selected oceanic gabbro samples. (a) (Crossed nicols, oil imm., scale bar = 50 μm). Ilmenite first and second generation trellis set along (111) planes of the magnetite host, which have resulted by oxidation - 'exsolution'. Locally developed fine grain magnetite - ilmenite, free of second ilmenite trellis (lower left corner) (b) (parallel nicols, oil imm., scale bar = 30 μm). Ilmenite first and second generation trellis (medium grey) set along (111) magnetite planes. Very fine rods of spinel (dark) exsolved along (100) planes of magnetite, partly enlarged by chemical destruction (black). At the contact between magnetite grain (most of the picture) and ilmenite grain (right side, homogeneous medium grey) a dotted rim of spinel, symplectitic intergrowth with ilmenite, develops; idem inside ilmenite lamellae. Regularly developed martite parallel to (111) planes (white rods). (c) (parallel nicols, oil imm., scale bar = 15 μm). Complex texture in a grain of ilmenite (sample 11A). Discontinuous oriented rods of magnetite, some of which changed to maghemite and to hematite (colour: from medium grey to light grey respectively). Spotty portions are ilmenite which has decomposed to fine hematite (light grey) and rutile (various medium greys). (d) (parallel nicols, oil imm., scale bar = 50 μm). Large skeletal to anhedral titanomagnetite with volume change cracks through which maghemitization starts, but unaltered core is left. Lath-shape skeletal ilmenite, at lower left corner (Sample 25F).

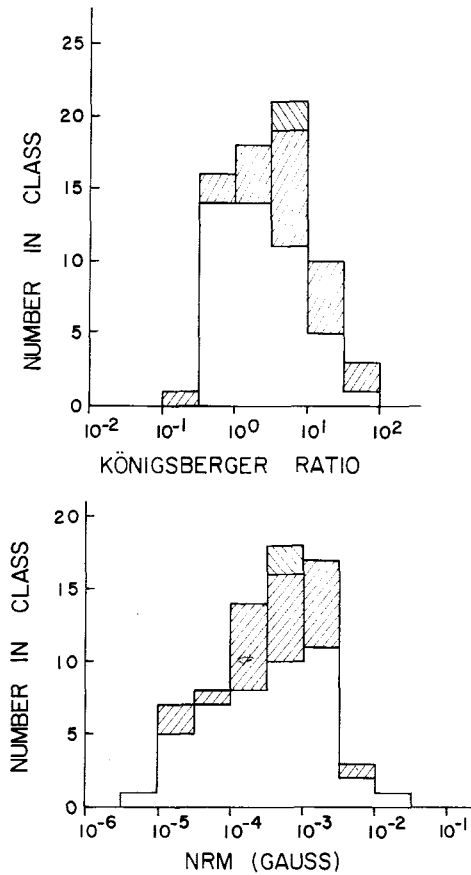


Figure 4. Frequency distributions of NRM intensities (bottom) and Königsberger ratio (top) in dredged oceanic gabbros. Unshaded area represents distribution ($N = 45$) determined in this study; diagonals to the left area represents distribution from study of Fox & Opdyke (1973) ($N = 22$); diagonals to the right area from Opdyke & Hekinian (1968) ($N = 2$).

are found to be quite variable. The intensities of NRM of the 45 gabbro samples studied here range over more than three orders of magnitude and follow on a logarithmic plot a distribution skewed toward higher values (Fig. 4). Fox & Opdyke (1973) reported remanent magnetic properties of 28 gabbroic samples dredged from the Kane fracture zone. The NRM intensities of their samples have a similar distribution to that present here (Fig. 4). Excluding six of their gabbroic samples which showed penetrative weathering, and including two dredged gabbro samples studied by Opdyke & Hekinian (1967), we calculate an overall ($N = 69$) geometric mean NRM intensity for available oceanic ridge gabbros of 3.47×10^{-4} G and an arithmetic mean intensity of 13.2×10^{-4} G. However, one sample we studied (at 77L; Table 2) has an intensity of NRM up to two orders of magnitude greater than these mean values; eliminating this sample gives recalculated values of 2.79×10^{-4} G and $8.79 (\pm 12.7 \text{ SD}) \times 10^{-4}$ G for the geometric and arithmetic means, respectively, which are considered more representative of oceanic gabbro magnetization.

The Königsberger ratio (Q_n) is a measure of the relative importance of remanent to induced magnetizations in a sample and is defined as:

$$Q_n = J_{\text{NRM}}/kF$$

where J_{NRM} is the intensity of NRM, k is the initial susceptibility and F is the geomagnetic field intensity (1965 IGRF) at the dredge locality. The calculated values of the Königsberger ratio for the 45 gabbro samples studied here, the 22 unweathered samples from Fox & Opdyke (1973) and the two gabbro samples from Opdyke & Hekinian (1967) follow an approximately log-normal distribution (Fig. 4). The geometric mean and arithmetic mean Königsberger ratio for these data are 3.1 and 8.1, respectively, again after excluding an abnormally high sample value. Therefore, on average, remanent magnetization dominates the total magnetization of these gabbros in the Earth's magnetic field, although, for 25 per cent of the samples, induced magnetizations are more important.

It is clear from inspection of Table 2 and the data in Fox & Opdyke (1973) that a large part of the variation in NRM intensity and in Königsberger ratio apparent in Fig. 4 arises from variations in remanent magnetic properties within each dredge haul. For example, the NRM intensities of nine gabbro samples from V30D18 range from 0.15 to 79.8×10^{-4} G. This within-site variation corresponds almost to the entire range of NRM intensity values observed for the 69 oceanic gabbro samples from a total of 18 dredge hauls. Further, we often observed a large variation in magnetization (NRM intensity and susceptibility) as well as opaque mineralogy content in specimens taken from a single sample. These observations suggest that the oceanic gabbros are not very homogeneously magnetized even on a hand-sample scale, as a result of different local concentrations of magnetic minerals.

Low-grade metamorphism has been found to lower the magnetization of oceanic basalts markedly (Opdyke & Hekinian 1967, Luyendyk & Melson 1967 and Irving, Robertson & Aumento 1970). However, data from the samples studied by Fox & Opdyke (1973) suggested that metamorphism and cataclasis do not appreciably alter the magnetic

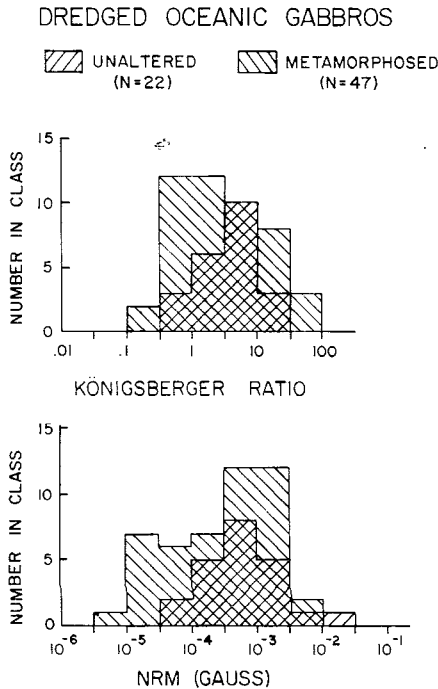


Figure 5. Comparison of frequency distributions of NRM intensities (bottom) and Königsberger ratios (top) of unaltered and metamorphosed dredged oceanic gabbros, using the sample values ($N = 69$ total) plotted in Fig. 4.

characteristics of gabbro in comparison to those of unaltered gabbro. We divided the data for the total of 69 gabbro samples into two populations: the first representing gabbros that can be considered essentially unaltered and the second representing gabbros which show evidence of metamorphism and/or cataclasis. The distributions of NRM intensity and Königsberger ratio for the two populations are compared in Fig. 5. Although the distributions of each parameter for the two types of gabbro are quite similar, with large overlaps in range, the metamorphosed gabbros have relatively higher frequencies at the lower range of values of NRM intensity and Königsberger Ratio, giving more skewed distributions as well as lower mean values (Table 3). It is important to note, however, that metamorphosed gabbros often have values of NRM intensity and Königsberger ratios that are as high as for the unaltered gabbros and the difference in mean values is at most a factor of two³ for the geometric mean while the arithmetic means are nearly equal (Table 3). These data suggest that, on average, metamorphism and cataclasis may result in lower remanent magnetizations

Table 3. Magnetization of oceanic igneous rocks.

	NRM (10^{-4} G)			Königsberger ratio		
	N	G.M.	A.M.	N	G.M.	A.M.
Basalt ¹						
dredged	311	55.8	144.0	304	31.5	98.5
DSDP	301	25.3	40.4	269	5.24	9.15
Metamorphosed basalt ²	16*	0.062	0.122	15*	0.49	1.55
Unaltered gabbro ³	21*	4.22	8.41	21*	3.58	5.05
Metamorphosed/cataclastic gabbro ³	47	2.32	8.96	47	2.95	9.39
All gabbros ³	68*	2.79	8.79	68*	3.13	8.05
Serpentinites ⁴	9	34.7	47.6	8	8.80	13.9

* One sample with magnetization two to three orders of magnitude greater than mean value not included. Compiled from data in: (1) Lowrie (1977); (2) Opdyke & Hekinian (1967), Luyendyk & Melson (1967), Irving *et al.* (1970), Fox & Opdyke (1973); (3) this study, Opdyke & Hekinian (1967), Fox & Opdyke (1973); (4) Opdyke & Hekinian (1967), Irving *et al.* (1970), Fox & Opdyke (1973).

of oceanic gabbros but certainly not to the degree and uniformity that has been observed for oceanic basalts. These observations are in accord with the studies of Ade-Hall, Palmer & Hubbard (1971) who found that rocks of basaltic composition that have undergone a high degree of deuteric oxidation, such as the oceanic metagabbros, appear to be relatively magnetically immune to moderate alteration.

3.2 STABILITY OF NRM

The change in direction and intensity of NRM with progressive AF demagnetization of representative gabbro samples is illustrated in Fig. 6. Although a small percentage of the samples possessed large low coercivity components of magnetization, most of the gabbro samples studied were characterized by highly stable remanences. That is, the directions of magnetization do not change significantly and the remanent intensities decrease slowly with demagnetization to fields of up to 800 Oe. From the AF demagnetization curves of the

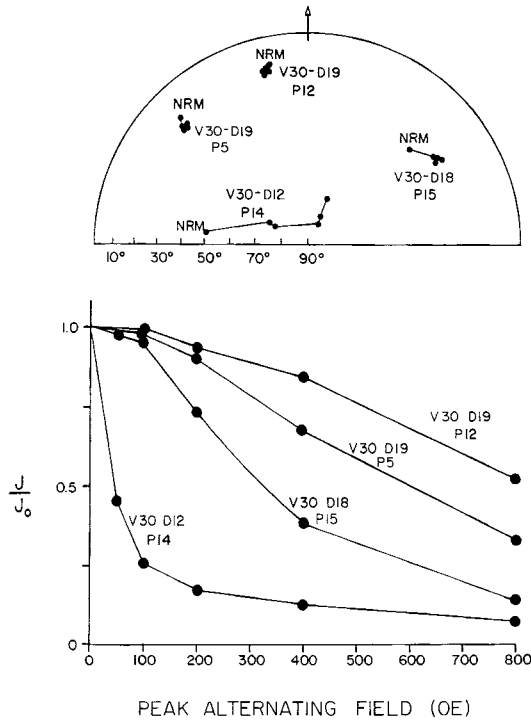


Figure 6. Representative AF demagnetization characteristics of NRM of dredged oceanic gabbro samples. Remanent directions plotted on stereographic projection are with respect to an arbitrary reference in each sample. J/J_0 is the fraction of the original NRM remaining after each demagnetization step.

gabbro samples studied here and those reported by Opdyke & Hekinian (1967) and Fox & Opdyke (1973), we calculated the magnitudes of the peak alternating field required to reduce the NRM intensity to one-half of its initial value. This parameter, the median destructive field, is a measure of the stability of remanent magnetization. The distribution of median destructive fields is strongly skewed toward high values (Fig. 7); of the total of

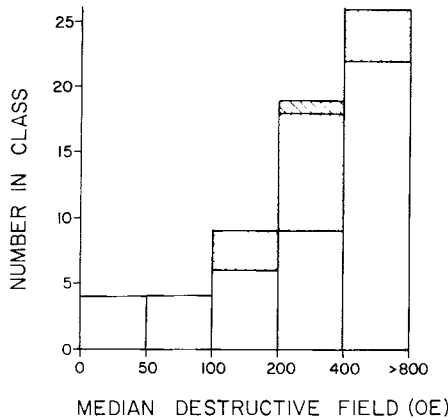


Figure 7. Frequency distribution of median destructive field of NRM of dredged oceanic gabbros calculated from AF demagnetization decay curves. Shading of areas the same as in Fig. 4.

62 oceanic gabbro samples for which AF demagnetization data is available, almost 75 per cent (45 samples) have median destructive fields greater than 200 Oe.

3.3 ORIGIN OF MAGNETIZATION IN OCEANIC GABBROS

Despite the large grain size in oceanic gabbros, the high remanent stability strongly suggests that the dominant magnetic mineral, magnetite, is fine-grained, possibly in the size range of a single domain behaviour. This inference is supported by the fine-grained pattern (Fig. 8) obtained in a test of dominant magnetic-domain state according to Lowrie & Fuller (1971) and Johnson, Lowrie & Kent (1975). High magnetic stability in coarse-grained basic intrusive rocks has been noted previously, by e.g. Evans & McElhinny (1969) in the Modipe gabbro, and Hargraves & Young (1969) in the Lambertville diabase. Strangway, Larson & Goldstein (1968) and Larson *et al.* (1969) have argued that the effective subdivision of larger grains into two exsolved phases, as the result of high-temperature deuteric oxidation of the originally homogeneous titanomagnetite, can result in small elongated regions of magnetite separated by intersecting ilmenite lamellae; in favourable cases these regions of magnetite may possess single-domain behaviour and carry a very stable thermoremanent magnetization. In the oceanic gabbro samples studied here by reflected-light microscopy, magnetite grains with abundant ilmenite lamellae were observed. It is, therefore, likely that the high magnetic stability of the oceanic gabbros can be attributed, at least in part, to the mechanism of titanomagnetite grain subdivision outlined above. It also has been observed that very fine grains of magnetite may occur exsolved in some silicate minerals, such as in pyroxene (Evans & McElhinny 1969), and plagioclase feldspars (Hargraves & Young 1969). Very fine grains of magnetite were observed in pyroxenes in some of our oceanic gabbro samples and such a manner of occurrence of magnetite provides an additional possible source of a stable remanence in these rocks. Since the formation of ilmenite lamellae and the subdivision of initially large, homogeneous titanomagnetite grains should occur at temperatures above the Curie point of magnetite (Buddington & Lindsley 1964), the magnetization of samples exhibiting these mineralogical features may represent a stable thermoremanent

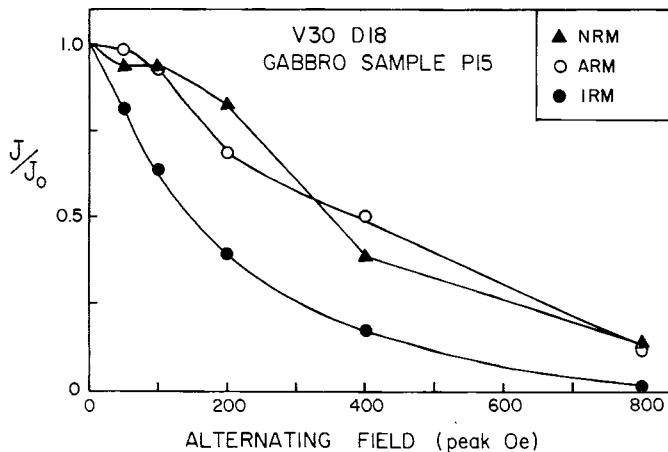


Figure 8. Comparison of AF demagnetization of NRM, ARM and IRM in an oceanic gabbro sample. ARM (anhysteretic remanent magnetization) was produced in a 1 Oe direct field coaxial with a 2000 Oe peak alternating field; IRM (isothermal remanent magnetization) was produced in a 7000 Oe direct field. J/J_0 is the fraction of initial remanent magnetization remaining after each demagnetization step.

magnetization (TRM) acquired during the initial cooling of the gabbro. Similarly, exsolved magnetite within crystals of plagioclase and pyroxene, which are of primary igneous origin, can also be expected to carry a stable primary TRM.

It has also been recognized that magnetite can occur as the result of subsequent alteration of the original rock. For example, magnetite inclusions have been found within actinolite, a metamorphic mineral (Evans & McElhinny 1969) and magnetite can be a byproduct in the oxidation of olivine (Watkins & Haggerty 1967; Hoye & O'Reilly 1973; Hoye & Evans 1975). Actinolite and serpentinized olivine with visible blobs of opaque minerals, including magnetite, associated with them, are present in several of the oceanic gabbro samples we have studied. Since those minerals can form at temperatures below the Curie point of magnetite, it is possible that the magnetization of some of the oceanic metagabbros is of thermochemical origin, acquired at about their time of metamorphism. Most of the metagabbros studied here are dominated by primary silicate and opaque minerals suggesting that the net magnetization of the rock is predominantly a function of primary TRM. We consider it unlikely that secondary magnetizations of the metagabbros, acquired during greenschist facies metamorphism of the gabbro body, contribute significantly to the magnetic properties of the gabbroic samples studied. This inference is supported by laboratory experiments which failed to identify any consistent secondary magnetization that could be related to the metamorphism: the majority of the metagabbro samples have a very stable univectorial NRM carried over a wide range of coercivities. If there is a contribution to the magnetic remanence of the metagabbros due to metamorphism, we suggest that this alteration took place shortly after crystallization of the gabbroic body before the occurrence of any significant changes in the relative orientation of the geomagnetic field. Consequently, magnetizations associated with metamorphic processes would be nearly parallel to the original TRM direction. With these results in mind, we contend that the gabbroic rocks of the oceanic crust preserve a record of the palaeomagnetic field acquired near to the time of crystallizations at the spreading axis.

3.4 COMPARISON OF GABBRO MAGNETIC PROPERTIES WITH OTHER OCEANIC ROCKS

Of the various rock types thought to constitute a portion of the oceanic crust, the most thoroughly studied, in terms of magnetic properties, are oceanic basalts, largely as the result of samples obtained by the Deep Sea Drilling Project; these data have been summarized by Lowrie (1974, 1977). Low-grade metamorphosed basalts, which may be representative of the lower part of Layer 2 (Fox, Schreiber & Peterson 1973), have been sampled on a number of dredging attempts. Remanent magnetic properties of samples of metamorphosed basalts have been reported in the studies of Opdyke & Hekinian (1967); Luyendyk & Melson (1967); Irving *et al.* (1970) and Fox & Opdyke (1973). Finally, the remanent characteristics of a handful of dredged serpentinized peridotite samples have been reported by Opdyke & Hekinian (1967), Irving *et al.* (1970) and Fox & Opdyke (1973). Serpentinized peridotite may constitute a small fraction of oceanic Layer 3 (Christensen 1972) or may be associated with, or be a product of, the tectonics of fracture zones (Fox & Opdyke 1973; Fox *et al.* 1976; Bonatti 1976).

The magnetic minerals in oceanic basalts are predominantly titanomagnetites with varying amounts of conversion to titanomaghemites. Largely as the result of rapid quenching, oceanic basalts mostly conform to deuteric oxidation class I (Wilson & Watkins 1967; Wilson, Haggerty & Watkins 1968) and are subsequently maghematized as a result of ocean-floor weathering or hydrothermal alteration. Curie temperatures of oceanic basalts typically

lie in the range 200–400°C (Lowrie 1974). In contrast, oceanic gabbros are characterized by a high deuteric oxidation state, with common formation in titanomagnetites of ilmenite lamellae and, in some cases, rutile, sphene and martite alteration assemblages. The dominant magnetic mineral in oceanic gabbros is magnetite, with Curie temperatures typically around 575°C. This magnetic mineralogy of oceanic gabbros is consistent with that expected for a slowly cooled mafic plutonic rock.

The magnetic mineralogy of oceanic metamorphosed basalts and serpentinized peridotites are poorly known. For oceanic metamorphosed basalts, a wide range of magnetic and mineralogical properties can be expected due to the combined action of two common processes, deuteric oxidation and hydrothermal alteration, as was found to be the case in subaerially exposed basaltic lavas (Ade-Hall *et al.* 1971). Serpentinized peridotites can be expected to contain magnetite, occurring in various concentrations and grain sizes, that formed during the serpentinization process (Saad 1969).

The mean magnetization intensities of the various oceanic crustal rock types have been obtained from values reported in the literature (Table 3). As has been observed previously by others, oceanic basalts as a whole are the most highly magnetized rocks in the oceanic crust. Dredged basalts typically have greater remanent intensities than DSDP basalts, most likely because the dredge collection represents younger and fresher rock (Lowrie 1974). The limited number of oceanic serpentinite samples give mean remanent intensities and Königsberger ratios that are of comparable magnitude to those of DSDP basalts.

Oceanic gabbros have NRM intensities that are on average about an order of magnitude less than those for the basalts and serpentinites. However, if arithmetic means are compared, the oceanic gabbros are only about a factor of 5 less intensely magnetized. The magnitudes of the Königsberger ratio for the basalt, serpentinite and gabbro collections indicate that remanent magnetizations in general equal or exceed magnetizations induced in the Earth's magnetic field in these rocks.

Metamorphosed basalts have the lowest remanent intensities and Königsberger ratios of the oceanic crustal rocks considered here. NRM intensities are at least one order of magnitude below those of gabbros and several orders of magnitude less than for the basalts. In contrast, metamorphosed gabbros have comparable magnetizations to unaltered gabbros.

On the basis of resistance to AF demagnetization, oceanic gabbros possess remanences that are remarkably stable, on average more so even than oceanic basalts. Whereas about 35 per cent of DSDP basalt samples have median destructive fields greater than 200 Oe (Lowrie 1974), the corresponding figure for oceanic gabbros is 70 per cent. The limited amount of magnetic stability data for metamorphosed basalts and serpentinites from the oceans suggest that the former are characterized by poor stability, while the latter may have NRM with moderate to high stability against AF demagnetization (Fox & Opdyke 1973).

4 Distribution of rock types and magnetization of the oceanic crust

In Fig. 9 we present a generalized model of the crustal stratigraphy of the oceanic crust. The upper portion of the crust is defined as seismic Layer 2A, and is known to be characterized by low compressional wave velocities (2.5–4.0 km/s), and has an average thickness of 500 m (Talwani *et al.* 1971; Houtz & Ewing 1976). Direct sampling of Layer 2A during Leg 37 of the Deep Sea Drilling Project indicates that the upper 500 m of the crust is comprised of a thin, fractured, chaotic pile of quickly chilled, glassy pillow basalts, basalt flows, shallow intrusives, intercalated sediments and void space. The physical properties of Layer 2A have been shown, however, to be time dependent. Houtz & Ewing (1976) showed

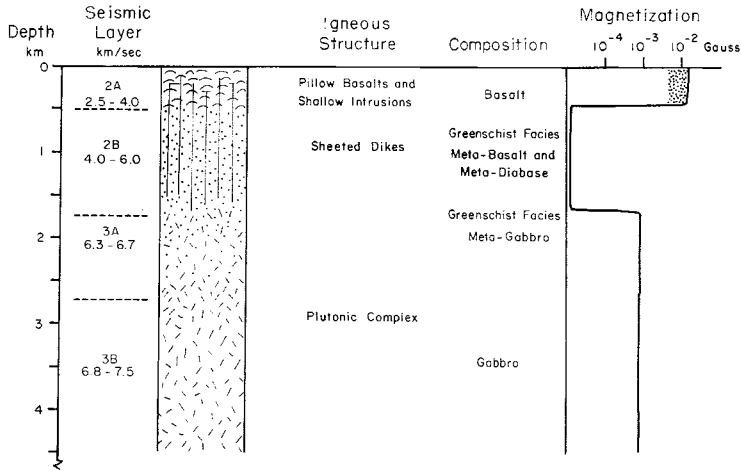


Figure 9. Generalized seismic, geologic and bulk remanent magnetization model of the oceanic crust (see text on constraints on the model). The column depicting the change in natural remanent magnetization with depth is based on a synthesis of the magnetic properties defined in rock types recovered from the ocean floor (Table 3 and text); shaded region represents decrease in remanent magnetization of Layer 2A as a result of progressive sea-floor weathering.

that the compressional wave velocity of Layer 2A increases with distance away from the accreting plate margins. These authors, along with Schreiber & Fox (1976, 1977) and Hyndman & Drury (1976), suggested that the cracks and void spaces of Layer 2A fill with low-temperature minerals precipitated during the cycling of water through the permeable Layer 2A carapace. As a result of this process Layer 2A becomes sealed and transmits seismic waves at a higher velocity.

The lower portion of oceanic basement is defined seismically as Layer 2B, has a compressional wave velocity range of 4.0–6.0 km/s and is thought to be predominantly comprised of sheeted dikes composed of zeolite and greenschist facies metamorphosed basalts and diabase (e.g. Cann 1970; Fox *et al.* 1973; Peterson, Fox & Schreiber 1974; Christensen & Salisbury 1975). Presumably, shortly after emplacement and crystallization of the basaltic margins along a dike conduit, the hot rock reacts with, and is altered by, the circulation of sea water which is fluxing through the upper few kilometres of the oceanic crust along permeable cracks and fissures (faults, dike chill margins, etc.). Support for this process of hydrothermal alteration has come from studies based on conductive heat flow measurements located near the axis of the Mid-Oceanic Ridge system (e.g. Talwani *et al.* 1971; Lister 1972; Hyndman & Rankin 1972; Anderson 1972; Sclater & Klitgord 1973; Williams *et al.* 1974; Anderson & Hobart 1976; Anderson, Langseth & Sclater 1977), from studies of ophiolite assemblages (e.g. Moores & Vine 1971; Gass & Smewing 1973; Stern, de Wit & Lawrence 1976), and from the geochemical character of greenschist facies rocks from the ocean floor and ophiolites (e.g. Muehlenbachs & Clayton 1972; Spooner & Fyfe 1973; Stern *et al.* 1976).

Layer 3 of the oceanic crust, often called the Oceanic Layer, is characterized by a wide spectrum of velocities ranging from 6.0 to 7.5 km/s. Recent studies indicate that the oceanic layer may be best described as two layers: Layer 3A characterized by a velocity range of 6.3–6.7 km/s and Layer 3B characterized by a velocity range of 6.8–7.5 km/s (e.g. Maynard 1970; Sutton, Maynard & Hussong 1971). Layer 3A probably represents that portion of the plutonic foundation of the oceanic crust which has experienced low-temperature greenschist

facies alteration as a result of the fluxing by hydrothermal fluids through interconnected crack systems that penetrate to depth from the sea-floor. Layer 3A is probably comprised principally of greenschist facies metagabbro. Layer 3B represents the lower portion of the plutonic complex which has been relatively unaffected by hydrothermal alteration and is characterized by unaltered gabbro of wide-ranging composition. Support for this model comes from the correlation of velocities measured by seismic refraction methods with laboratory determined velocities of rocks recovered from the ocean floor and ophiolites (e.g. Fox *et al.* 1973; Peterson *et al.* 1974; Christensen & Salisbury 1975), from inferences based on the location of metagabbros with respect to ocean-floor topography (Bonatti *et al.* 1975) and from studies of ophiolite assemblages (e.g. Cann 1970; Gass & Smewing 1973; Stern *et al.* 1976).

The generalized model of the crustal stratigraphy of the oceanic crust implies that serpentinized peridotite does not comprise a significant portion of the oceanic crust accreted along the axis of the Mid-Oceanic Ridge system. Locally, however, serpentinite may be an important constituent of the oceanic crust. It has been shown that serpentinite can characterize large portions of fracture zone terrain (e.g. Miyashiro, Shido & Ewing 1969; Bonatti, Honnorez & Ferrara 1971; Melson & Thompson 1971; Bonatti & Honnorez 1976; Fox *et al.* 1976) and Aumento & Loubat (1971) and Bonatti (1976) present evidence which suggests that serpentinite bodies migrate diapirically along faults parallel to the accreting plate margins, resulting in thin, near-vertical screens of serpentinite.

Given the validity of the generalized model of oceanic crustal structure outlined in the preceding paragraphs, and accepting the proposition that the samples chosen for magnetic property analysis are representative rock bodies found within the oceanic crust, then the constraints needed to propose a working model for magnetization distribution in the oceanic crust are available. The upper 500 m of the oceanic crust (approximately equivalent to seismic Layer 2A) is characterized by strongly magnetized basalts. As for other physical properties, the magnetic properties of this quickly chilled volcanic carapace are also time dependent. In particular, the intensity of NRM decreases rapidly within several million years after cooling at the spreading axis of the mid-ocean ridge and this variation has been shown to be largely a function of the low-temperature weathering of the basalt and the conversion of titanomagnetite to titanomaghemite (Irving 1970; Irving *et al.* 1970; Marshall & Cox 1972; Johnson & Atwater 1977). We consider the arithmetic mean values for NRM of 144×10^{-4} G for dredged basalts and of 40×10^{-4} G for DSDP basalts (Table 3) to be representative of the change in NRM intensity from young and fresh to older and more weathered oceanic basalts. Weakly magnetized (0.122×10^{-4} G) greenschist facies metabasalts and metadiabase underlie the strongly magnetized basaltic carapace and comprise the sheeted dike complex (Layer 2B). Finally, the plutonic foundation of the oceanic crust underlies the sheeted dikes and is composed predominantly of gabbroic rocks. The greenschist facies metagabbro found in abundance in the upper portion of the oceanic layer (Layer 3A) is characterized by moderate NRM intensities (arithmetic mean 8.96×10^{-4} G); unaltered gabbro, found in abundance in the lower portion of the oceanic layer (Layer 3B), is also characterized by moderate NRM intensities (arithmetic mean 8.71×10^{-4} G). Note that magnetizations assigned to the crustal layers are arithmetic, rather than geometric, mean values calculated for the appropriate rock types since the former statistic is more relevant in determining the contribution to magnetic anomaly amplitudes (Harrison 1976). There is the problem, however, of even one high value strongly biasing the arithmetic mean which we try to minimize by excluding the uncharacteristic samples from the calculations of the means (Table 3).

We consider rock units below the gabbroic layer, in the upper mantle, to have a negligible

remanent magnetization and thus not to be involved directly in producing sea-floor spreading magnetic anomalies. The remanent magnetic properties of ultramafic rocks such as dunites, peridotites and pyroxenites, the probable constituents of the upper mantle, are acquired primarily during the process of serpentinization (Saad 1969) which is unlikely to occur in the mantle. However, although we do not consider serpentinite to comprise a significant portion even of the oceanic crust, it is quite likely that local concentrations of the highly magnetic serpentinite, such as along fracture zones and normal faults in the oceanic crust, may have a pronounced magnetic signature (Bonatti 1976).

This model of the magnetization distribution in the oceanic crust inferred from the magnetic properties of dredged oceanic rocks is compatible with the magnetic properties observed in ophiolites. Ophiolites may represent obducted sections of oceanic crust and consist of a pseudostratiform sequence of ultramafics, gabbro, sheeted dikes, pillow basalt and deep-sea sediments (e.g. Gass 1968; Moores & Vine 1971). In the Troodos Complex, Cyprus, the NRM intensity is on the order of 10^{-2} G for both the pillow basalts and serpentinized peridotites, and on the order of 10^{-3} G for the gabbros and sheeted dike rocks (Vine & Moores 1972). However, only the pillow basalts and gabbros yield consistent NRM directions, well away from the present geomagnetic field direction in Cyprus; the non-remobilized serpentinized peridotites have remanent directions along the present magnetic field while the remanent directions of the greenstones from the sheeted dikes are intermediate between those of the pillow basalts and gabbros and the present direction of the Earth's magnetic field (Moores & Vine 1971). The stability of remanence inferred from these relations in the Troodos units is comparable to the remanent stabilities characterized by AF demagnetization of correlative rock types dredged and drilled from the oceans. The pillow basalts and gabbros from Troodos and the ocean floor preserve to a large degree their primary thermoremanent magnetization directions, whereas the metamorphosed basalts carry large secondary components of magnetization. The stable remanent magnetization in some serpentinized peridotites can be attributed to a chemical remanence acquired during serpentinization (Saad 1969). In the Troodos Complex, the direction of magnetization suggests that serpentinization is related to the late Tertiary uplift and emplacement of the massif rather than to the formation of this segment of oceanic crust in the Cretaceous (Moores & Vine 1971).

5 Contribution of source layers to magnetic anomalies

On the basis of the magnetization distribution inferred from the magnetic properties of dredged and drilled oceanic rocks, we suggest that in addition to the highly magnetized basalts of Layer 2A, magnetization contrasts in the presumed great thickness of gabbros thought to comprise Layer 3 can be expected to contribute significantly to lineated marine magnetic anomalies. In contrast, because of their weak remanent intensities and poor stabilities, metamorphosed basalts and diabase thought to lie in the lower part of Layer 2 would contribute very little.

We have calculated the magnitude of the expected anomaly from a source situated in Layer 3 of the oceanic crust and compared it to the contribution from a Layer 2A source using simple two-dimensional magnetic models (Fig. 10). In the Layer 3 models, the source body is assumed to be a plane layer with the upper surface at a depth of 7.5 km below sea level and with a nominal thickness of 4.5 km. The magnetic field and remanent vectors are made vertical and the value for the remanent magnetization is 0.0008 G (arithmetic mean value for dredged oceanic gabbros; Table 3), giving a magnetization contrast between oppositely polarized blocks within the layer of twice the value or 0.0016 G. For the

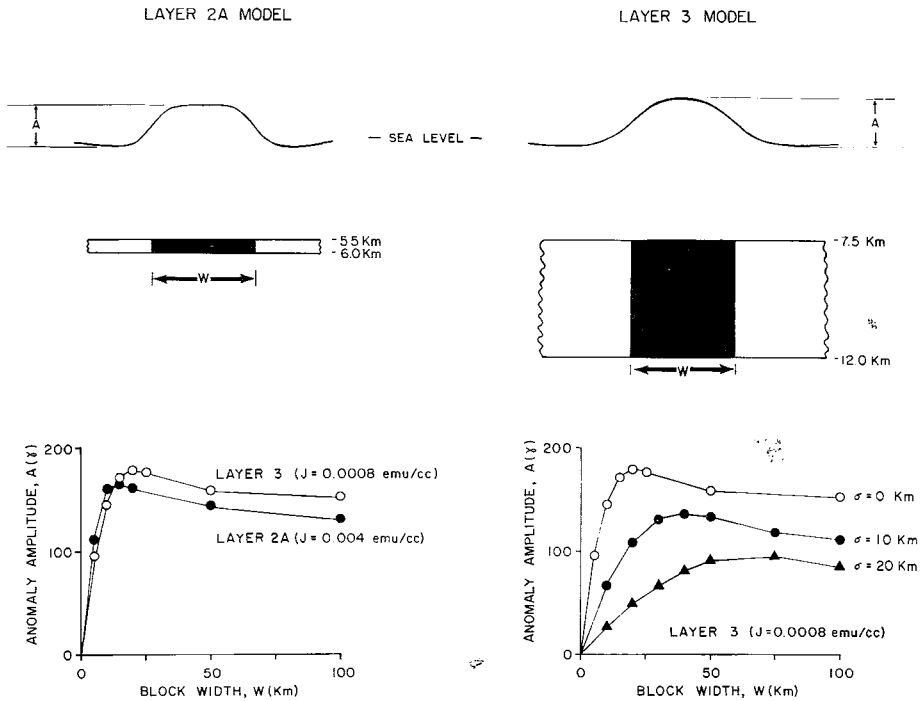


Figure 10. Models calculated at the pole (i.e. remanent and field vectors vertical) for two-dimensional models of Layer 2A source and Layer 3 source with shaded (unshaded) area corresponding to normal (reversed) polarity. Lower left: Comparison of peak to peak magnetic anomaly amplitudes against block width for Layer 2A and Layer 3 sources. Lower right: Peak to peak magnetic anomaly amplitudes against block width for different widths of transition zones in Layer 3 source. Transition zone width is specified by the standard deviation, σ , of the Gaussian magnetization distribution between oppositely polarized source blocks. Graph for $\sigma = 0$ km corresponds to Layer 3 curve in graph at lower left.

Layer 2A models, a 0.5 km thick plane layer with its upper surface at 5.5 km depth and a remanent magnetization of 0.004 G (arithmetic mean value for DSDP basalts; Lowrie 1977; Table 3) is used. The peak to peak magnetic anomaly is plotted against the width of the source block for both a Layer 2A source and a Layer 3 source in Fig. 10(a).

From these model calculations, it is apparent that magnetization contrasts in Layer 3, corresponding to the measured magnetic properties of oceanic gabbros, give magnetic anomaly amplitudes comparable to those for a Layer 2A source. Although the magnetization inferred for Layer 3 is about a factor of 5 lower than for Layer 2A and resides deeper in the oceanic crust, this is, in good part, compensated for in producing an anomalous field by the much greater thickness of the Layer 3 source. We note also that the maximum amplitude of the anomaly occurs at a greater block width for the Layer 3 model in comparison to the Layer 2A model. This is simply due to the greater source depth of Layer 3 and implies that, with all other factors the same, the relative contribution from this deeper source, and hence the magnitude of the magnetic anomaly due to the combined effects of Layer 2A and Layer 3 sources can be expected to be at a maximum when the typical widths of the polarized crustal blocks are about 15 km.

Not taken into account in these model calculations, which suggest comparable anomaly amplitude contributions, are possible differences in the widths of the transition zones between oppositely polarized blocks in the Layer 2A and the Layer 3 source regions. It is

quite likely that the transition zones are generally narrow in Layer 2A, on the order of a few kilometres and less (Atwater & Mudie 1973), due in large part to the rapid acquisition of the remanent magnetization by the predominantly extrusive pillow basalts from the time of their emplacement at the spreading ridge axis. This is in contrast to the relatively wide transition zones that are probably characteristic of Layer 3 in which the acquisition of remanence in the more slowly cooled plutonic rocks might be delayed progressively with depth along sloping isotherms (Cande & Kent 1976; Blakely 1976) and also possibly offset because of the width of a magma chamber.

We have modelled the transition zones in general terms as a lateral magnetization variation corresponding to a Gaussian distribution, following the techniques of Schouten & McCamy (1972). The width of the transition zone can be specified by the standard deviation (σ in km) of the Gaussian distribution. This means that 68 per cent of the change in magnetization from $+J$ to $-J$ occurs over a lateral distance of 2σ km, or 95 per cent over 4σ km. The peak to peak anomaly amplitude is plotted against block width for a Layer 3 source with values of σ equal to 10 and 20 km and these are compared to the variation in anomaly amplitude corresponding to an infinitesimally thin transition zone (i.e. $\sigma=0$ km) in Fig. 10(b). The effect of increasing the width of the transition zone between the apparently polarized source blocks is primarily a decrease in the amplitude of the magnetic anomaly. In addition to this, the variation in anomaly amplitude with block width is such that the maximum anomaly occurs at larger block widths for increasing values of transition zone width. For example, the maximum anomaly amplitude for a Layer 3 source with transition zones of $\sigma=10$ km occurs at a block width of about 40 km compared to a block width of about 15 km for $\sigma=0$. However, it is apparent that the anomaly produced by a Layer 3 source with relatively wide transition zones is still comparable to the anomaly resulting from a Layer 2A source, according to the assumptions made here for depths and magnetization values.

6 Summary and discussion

Oceanic gabbros dredged from equatorial Atlantic Ocean fracture zones were found to have stable remanent magnetizations that are of moderate intensity. Magnetic and mineralogical evidence suggest the magnetization of the gabbros is dominated by a TRM or possibly a thermochemical remanence carried by magnetite and probably acquired during initial cooling from the time of emplacement. If the dredged gabbros are representative of the dominant lithology of Layer 3 of the oceanic crust, and if a substantial portion of this gabbroid layer is emplaced near to the spreading ridge axis, then on the basis of the magnetic properties a record of geomagnetic reversals should be preserved in this layer and be reflected as a significant contribution to the lineated marine magnetic anomalies, normally thought to originate primarily from Layer 2A.

The possible presence of an additional magnetic source layer at depth in the oceanic crust adds some complexity to the interpretation of marine magnetic anomalies, but at the same time may account for certain features. For the latter, the apparent discrepancy between measured magnetization values of DSDP basalts and the magnetization required to model magnetic anomaly amplitudes with a presumed single, thin (~ 0.5 km) Layer 2A source is largely removed if an additional contribution from a Layer 3 source is present. Other explanations to account for the apparent discrepancy are possible, such as a thicker basaltic (Layer 2A) source or a bias toward lower magnetizations in DSDP basalts due to non-representative sampling of Layer 2A. We suggest that a possibly small, but significant, contribution from Layer 3 is a viable alternative to these *ad hoc* explanations and that our proposition satisfies most of the relevant observations.

Unlike the time-dependent magnetization of Layer 2A, we expect the remanent magnetization of the Layer 3 gabbros and metagabbros to remain essentially unchanged from the time of acquisition near the spreading areas. This is because progressive sea-floor weathering, the process primarily responsible for the magnetic alteration of Layer 2A, is less apt to penetrate and to affect the deeper Layer 3 rocks; the general paucity of evidence for magnetization in the gabbro and metagabbro samples we have studied provides support for this supposition. The progressive diminution in the remanent magnetization of Layer 2A basalts has led to the suggestion that older magnetic anomalies originate predominantly from deeper sources, a subsidiary effect of which is the apparent suppression of records of shorter magnetic events, as in the lower Tertiary anomaly sequences (Blakely 1976). However, Larson, Cande & LaBrecque (1975) and Cande & Kent (1976) have presented evidence from the shapes of marine magnetic anomalies which suggests that a contribution from a source characterized by relatively sharp transition zones, such as is expected in Layer 2A, continues to dominate even in the Mesozoic anomaly sequence. This implies that the apparent lower frequency of geomagnetic reversals in the lower Tertiary, compared to the upper Tertiary, is real and not an artifact of decreased fidelity in the marine magnetic anomaly record, a conclusion supported by independent magnetic polarity determinations in stratigraphic sections spanning the Late Cretaceous and Early Palaeocene (Alvarez *et al.* 1977; Butler *et al.* 1977). A large part of the decrease in magnetization of Layer 2A basalts most likely occurs within a few million years of formation (Johnson & Atwater 1977) and Layer 2A continues to dominate, although in reduced proportion, as the source of marine magnetic anomalies in older oceanic crust (Cande & Kent 1976).

Although an additional (but subordinate) magnetic source layer in the oceanic crust does not necessarily affect the interpretation of marine magnetic anomalies as a record of geomagnetic field reversals *per se*, it can present some complications in attempts to derive more detailed information about palaeofield behaviour from the observed anomalies. For example, Schouten & Cande (1976) presented two quantitative methods for determining palaeomagnetic poles from the shape of marine magnetic anomalies. The theta method compares the skewness of two contemporaneous sets of anomalies on the same rigid plate while the amplitude factor method compares their relative amplitudes. Both methods are based on a simple model for the magnetic source — a single layer of constant thickness at constant depth consisting of two-dimensional blocks of constant magnetization and alternative polarity — and a geocentric axial dipole field. However, the additional presence of a deeper source layer could introduce significant errors in these methods.

Several studies have already indicated that there are systematic discrepancies between the observed skewness in the shape of some magnetic anomalies and the skewness predicted by the simple model (Weissel & Hayes 1972; Cande 1976). Cande & Kent (1976) have shown that a contribution from a deeper source layer with broad, sloping transition zones can account for some of these observations. The magnetic properties of oceanic gabbros, that may be representative of the assumed deeper source in Layer 3 reported here, are in good agreement with the characteristics assumed by Cande & Kent in modelling the magnetization distribution in the oceanic crust which can produce a skewness discrepancy that is unrelated to field behaviour or plate motion.

It is also apparent from the models in Fig. 10 that the amplitude ratio of contemporaneous sets of anomalies can be influenced by a deeper source layer if the two sets of anomalies were formed at different spreading rates. If the enhanced effect of a deeper source in more widely-spaced blocks of alternating polarity is not accounted for, the amplitude ratio may not simply reflect the latitudinal variation in the dipole palaeofield intensity which is a necessary assumption in the determination of palaeomagnetic poles from the

magnetic anomalies. For similar reasons, the determination of relative palaeomagnetic field intensity from the temporal variation of magnetic anomaly amplitudes is likely to be affected by the presence of a deeper source layer in the oceanic. This is because the geomagnetic reversal frequency has not been constant and unless anomalies of different age with a similar duration (assuming a constant spreading rate) are compared, variation with block width in the contribution from the deeper source could give anomaly amplitude variations that are less related to long-term changes in the palaeofield intensity than to differences in the geometry of the source bodies.

In conclusion, it is obvious that additional magnetic property data on oceanic gabbros, from a wider geographical and structural distribution, are required to assess the generality of our conclusions to the oceanic crust, particularly in light of the considerable range of magnetization values that appear to characterize the oceanic gabbros. Nevertheless, the available data from dredged gabbros, ophiolites and magnetic anomaly interpretations are consistent in indicating that the oceanic gabbroic layer is very likely to be an important source region for marine magnetic anomalies.

Acknowledgments

We thank S. C. Cande, W. Lowrie and P. D. Rabinowitz for reviewing the manuscript and offering helpful comments. We also thank Captain H. Kohler, the officers and crew of the R/V *Vema* for aiding in the collection of the samples used in this study.

This work was supported by National Science Foundation Grants OCE 76-21962 and OCE 75-21753 and NSF/IDOE Grant GX-40428. Support for the collection and curating facilities of the Lamont-Doherty Geological Observatory dredge collection is provided by the National Science Foundation, Grant OCE 76-18049 A01 and the Office of Naval Research, Grant N00014-75-C-0210 (Scope E).

Lamont-Doherty Geological Observatory Contribution No. 2715.

References

- Ade-Hall, J. M., Palmer, H. C. & Hubbard, T. P., 1971. The magnetic and opaque petrologic response of basalts to regional hydrothermal alteration, *Geophys. J. R. astr. Soc.*, **24**, 137–174.
- Alvarez, W., Arthur, M. A., Fischer, A. G., Lowrie, W., Napoleone, G., Premoli Silva, I. & Roggenthen, W. M., 1977. Upper Cretaceous–Paleocene magnetic stratigraphy at Gubbio, Italy. V. Type section for the late Cretaceous–Paleocene geomagnetic reversal time scale, *Geol. Soc. Am. Bull.*, **88**, 383–389.
- Anderson, R. N., 1972. Petrological significance of low heat flow on the flanks of slow-spreading midocean ridges, *Geol. Soc. Am. Bull.*, **83**, 2947–2956.
- Anderson, R. N. & Hobart, M. A., 1976. The relation between heat flow, sediment thickness, and age in the eastern Pacific, *J. geophys. Res.*, **81**, 2968–2989.
- Anderson, R. N., Langseth, M. G. & Sclater, J. G., 1977. The mechanism of heat transfer through the floor of the Indian Ocean, *J. geophys. Res.*, **82**, 3391–4409.
- Atwater, T. & Mudie, J. D., 1973. Detailed near-bottom study of the Gorda Rise, *J. geophys. Res.*, **78**, 8665–8686.
- Aumento, F. & Loubat, H., 1971. The Mid-Atlantic Ridge near 45° N: serpentinized ultramafic intrusions, *Can. J. Earth Sci.*, **8**, 631–663.
- Blakely, R. J., 1976. An age dependent, two-layer model for marine magnetic anomalies, *Am. Geophys. Un. Monogr.*, **19**, 227–234.
- Bonatti, E., 1976. Serpentinite protrusions in the oceanic crust, *Earth planet. Sci. Lett.*, **32**, 107–113.
- Bonatti, E. & Honnorez, J., 1976. Sections of the Earth's crust in the equatorial Atlantic, *J. geophys. Res.*, **81**, 4104–4116.
- Bonatti, E., Honnorez, J. & Ferrara, G., 1971. Peridotite-gabbro–basalt complex from the equatorial Mid-Atlantic Ridge, *Phil. Trans. R. Soc. Lond. A*, **268**, 385–402.

- Bonatti, E., Honnorez, J., Kirst, P. & Radicati, F., 1975. Metagabbros from the Mid-Atlantic Ridge at 06° N: contact-hydrothermal-dynamic metamorphism beneath the Axial Valley, *J. Geol.*, **83**, 61–78.
- Buddington, A. F., Fahey, J. & Vlisidis, A., 1963. Degree of oxidation of Adirondack iron oxide and non-titanium oxide minerals in relation to petrogeny, *J. Petrol.*, **4**, 138–149.
- Buddington, A. F. & Lindsley, D. H., 1964. Iron–titanium oxide minerals and synthetic equivalents, *J. Petrol.*, **5**, 310–357.
- Butler, R. F., Lindsay, E. H., Jacobs, L. L. & Johnson, N. M., 1977. Magnetostratigraphy of the Cretaceous/Tertiary boundary in the San Juan Basin, New Mexico, *Nature*, **267**, 318–323.
- Cande, S. C., 1976. A palaeomagnetic pole from Late Cretaceous marine magnetic anomalies in the Pacific, *Geophys. J. R. astr. Soc.*, **44**, 547–566.
- Cande, S. C. & Kent, D. V., 1976. Constraints imposed by the shape of marine magnetic anomalies on the magnetic source, *J. geophys. Res.*, **81**, 4157–4162.
- Cann, J. R., 1970. New model for the structure of the ocean crust, *Nature*, **226**, 928–930.
- Christensen, N. I., 1972. The abundance of serpentinites in the ocean crust, *J. Geol.*, **80**, 709–719.
- Christensen, N. I. & Salisbury, M. H., 1975. Structure and constitution of the lower oceanic crust, *Rev. Geophys. Space Phys.*, **13**, 57–86.
- Evans, M. E. & McElhinny, M. W., 1969. An investigation of the origin of stable remanence in magnetite bearing igneous rocks, *J. Geomag. Geoelect.*, **21**, 757–773.
- Fox, P. J. & Opdyke, N. D., 1973. Geology of the oceanic crust: magnetic properties of oceanic rocks, *J. geophys. Res.*, **78**, 5139–5154.
- Fox, P. J., Schreiber, E. & Peterson, J. J., 1973. The geology of the oceanic crust: compressional wave velocities of oceanic rocks, *J. geophys. Res.*, **78**, 5155–5172.
- Fox, P. J., Schreiber, E., Rowlett, H. & McCamy, K., 1976. The geology of the Oceanographer Fracture Zone: a model for fracture zones, *J. geophys. Res.*, **81**, 4117–4128.
- Gass, I. G., 1968. Is the Troodos massif of Cyprus a fragment of Mesozoic ocean floor? *Nature*, **200**, 39–42.
- Gass, I. G. & Smewing, J. D., 1973. Intrusion, extrusion and metamorphism at constructive margins: evidence from the Troodos massif, Cyprus, *Nature*, **242**, 26–29.
- Grommé, C. S., Wright, T. L. & Peck, D. L., 1969. Magnetic properties and oxidation of iron–titanium minerals in Aleo and Makaopuhi lava lakes, Hawaii, *J. geophys. Res.*, **74**, 5277–5293.
- Haggerty, S. E., 1976. Opaque mineral oxides in terrestrial igneous rocks, in *Oxide minerals*, ed. Rumble III, D., Miner. Soc. Am. Short Course Notes, **3**, 101–300.
- Hargraves, R. B. & Young, W. M., 1969. Source of stable remanent magnetism in Lambertville diabase, *Am. J. Sci.*, **267**, 1161–1177.
- Harrison, C. G. A., 1976. Magnetization of the oceanic crust, *Geophys. J. R. astr. Soc.*, **47**, 257–283.
- Hess, H. H., 1962. History of the ocean basins, in *Petrologic studies*, pp. 599–620, eds Engel, A. E. J., James, H. L. & Leonard, R. F., (Buddington Vol.), Geol. Soc. Am.
- Hess, H. H., 1965. Mid-ocean ridges and tectonics of the sea floor, pp. 317–333, *Colston Papers, Proc. 17th Symp. Colston Research Soc.*, University of Bristol, Butterworths.
- Houtz, R. & Ewing, J., 1976. Upper crustal structure as a function of plate age, *J. geophys. Res.*, **81**, 2490–2498.
- Hoye, G. S. & Evans, M. E., 1975. Remanent magnetization in oxidized olivine, *Geophys. J. R. astr. Soc.*, **41**, 138–151.
- Hoye, G. S. & O'Reilly, W., 1973. Low temperature oxidation of ferromagnesian olivines – a gravimetric and magnetic study, *Geophys. J. R. astr. Soc.*, **33**, 81–92.
- Hyndman, R. D. & Drury, M. J., 1976. The physical properties of oceanic basement rocks from deep drilling on the Mid-Atlantic Ridge, *J. geophys. Res.*, **81**, 4042–4052.
- Hyndman, R. D. & Rankin, D. S., 1972. The Mid-Atlantic Ridge near 45° N. 18. Heat flow measurements, *Can. J. Earth Sci.*, **9**, 664–670.
- Irving, E., 1970. The Mid-Atlantic Ridge at 45° N. XIV. Oxidation and magnetic properties of basalt; review and discussion, *Can. J. Earth Sci.*, **7**, 1528–1538.
- Irving, E., Robertson, W. A. & Aumento, F., 1970. The Mid-Atlantic Ridge near 45° N. VI. Remanent intensity, susceptibility, and iron content of dredged samples, *Can. J. Earth Sci.*, **7**, 226–238.
- Johnson, H. P. & Atwater, T., 1977. Magnetic study of basalts from the Mid-Atlantic Ridge, lat. 37° N, *Geol. Soc. Am. Bull.*, **88**, 637–647.
- Johnson, H. P., Lowrie, W. & Kent, D. V., 1975. Stability of anhysteretic remanent magnetization in fine and coarse magnetite and maghemite particles, *Geophys. J. R. astr. Soc.*, **41**, 1–10.
- Klitgord, K. D., Heustis, S. P., Mudie, J. D. & Parker, R. L., 1975. An analysis of near-bottom magnetic anomalies: sea-floor spreading and the magnetized layer, *Geophys. J. R. astr. Soc.*, **43**, 387–424.

- Larson, E., Ozima, M., Ozima, M., Nagata, T. & Strangway, D., 1969. Stability of remanent magnetization of igneous rocks, *Geophys. J. R. astr. Soc.*, **17**, 263–292.
- Larson, R. L., Cande, S. C. & LaBrecque, J. L., 1975. On the permanency of magnetic anomalies (abs), p. 60, *IUGG XVI General Assembly, Abstracts*, Grenoble, France, 1975.
- Lister, C. R. B., 1972. On the thermal balance of a mid-ocean ridge, *Geophys. J. R. astr. Soc.*, **26**, 515–535.
- Lowrie, W., 1974. Oceanic basalt magnetic properties and the Vine and Matthews hypothesis, *J. Geophys.*, **40**, 513–536.
- Lowrie, W., 1977. Intensity and direction of magnetization in oceanic basalts, *J. Geol. Soc.*, **133**, 61–82.
- Lowrie, W. & Fuller, M., 1971. On the alternating field demagnetization characteristics of multidomain thermoremanent magnetization in magnetite, *J. geophys. Res.*, **76**, 6339–6349.
- Luyendyk, B. P. & Melson, W. G., 1967. Magnetic properties of rocks near the crest of the Mid-Atlantic Ridge, *Nature*, **215**, 147–149.
- Marshall, M. & Cox, A., 1972. Magnetic changes in pillow basalt due to sea-floor weathering, *J. geophys. Res.*, **77**, 6459–6469.
- Maynard, G. L., 1970. Crustal layer of seismic velocity 6.9–7.6 kilometres per second under the deep oceans, *Science*, **168**, 120–121.
- Melson, W. G. & Thompson, G., 1971. Petrology of a transform zone and adjacent ridge segments, *Phil. Trans. R. Soc. Lond. A*, **268**, 423–441.
- Miyashiro, A., Shido, F. & Ewing, M., 1969. Composition and origin of serpentinites from the mid-Atlantic ridge near 24° and 30° north latitude, *Contr. Miner. Petrol.*, **23**, 117–127.
- Moores, E. M. & Vine, F. J., 1971. The Troodos Massif, Cyprus and other ophiolites as oceanic crust: evaluation and implications, *Phil. Trans. R. Soc. Lond. A*, **268**, 443–466.
- Muehlenbachs, K. & Clayton, R. N., 1972. Oxygen isotope geochemistry of submarine greenstones, *Can. J. Earth Sci.*, **9**, 471–478.
- Opdyke, N. D. & Hekinian, R., 1967. Magnetic properties of some igneous rocks from the Mid-Atlantic Ridge, *J. geophys. Res.*, **72**, 2257–2260.
- Ozima, M. & Ozima, M., 1971. Characteristic thermomagnetic curve in submarine basalts, *J. geophys. Res.*, **76**, 2051–2056.
- Peterson, J. J., Fox, P. J. & Schreiber, E., 1974. Newfoundland ophiolites and the geology of the oceanic layer, *Nature*, **247**, 194–196.
- Ryall, P. J. C., Hall, J. M., Clark, J. & Milligan, T., 1977. Magnetization of oceanic crustal layer 2 – results and thoughts after DSDP Leg 37, *Can. J. Earth Sci.*, **14**, 684–706.
- Saad, A. H., 1969. Magnetic properties of ultramafic rocks from Red Mountain, California, *Geophysics*, **34**, 974–987.
- Schouten, H. & McCamy, K., 1972. Filtering marine magnetic anomalies, *J. geophys. Res.*, **77**, 7089–7099.
- Schouten, H. & Cande, S. C., 1976. Palaeomagnetic poles from marine magnetic anomalies, *Geophys. J. R. astr. Soc.*, **44**, 567–575.
- Schreiber, E. & Fox, P. J., 1976. Compressional wave velocities and mineralogy of fresh basalts from the Famous area and the Oceanographer Fracture Zone and the texture of Layer 2A of the oceanic crust, *J. geophys. Res.*, **81**, 4071–4076.
- Schreiber, E. & Fox, P. J., 1977. Density and *P*-wave velocity of rocks from the FAMOUS region and their implication to the structure of the oceanic crust, *Geol. Soc. Am. Bull.*, **88**, 600–608.
- Sclater, J. G. & Klitgord, K. D., 1973. A detailed heat flow, topographic, and magnetic survey across the Galapagos spreading center at 86° W, *J. geophys. Res.*, **78**, 6951–6975.
- Spooner, E. T. C. & Fyfe, W. S., 1973. Sub-sea floor metamorphism, heat and mass transfer, *Contr. Miner. Petrol.*, **42**, 487–304.
- Stern, C., deWit, M. J. & Lawrence, J. R., 1976. Igneous and metamorphic processes associated with the formation of Chilean ophiolites and their implication for ocean floor metamorphism, seismic layering and magnetism, *J. geophys. Res.*, **81**, 4370–4380.
- Strangway, D. W., Larson, E. E. & Goldstein, M., 1968. A possible cause of high magnetic stability in volcanic rocks, *J. geophys. Res.*, **73**, 3787–3795.
- Sutton, G. H., Maynard, G. L. & Hussong, D. M., 1971. Widespread occurrence of a high-velocity basal layer in the Pacific crust found with repetitive sources and sonobuoys, in *The structure and physical properties of the Earth's crust*, pp. 193–209, Geophys. Monogr. Ser., vol. 14, ed. Heacock, J. G., AGU, Washington, DC.
- Talwani, M., Windisch, C. C. & Langseth, M. G. Jr. 1971. Reykjanes Ridge Crest: a detailed geophysical study, *J. geophys. Res.*, **76**, 473–517.

- Vine, F. J. & Matthews, D. H., 1963. Magnetic anomalies over oceanic ridges, *Nature*, **199**, 947–949.
- Vine, F. J. & Moores, E. M., 1972. A model for the gross structure, petrology, and magnetic properties of oceanic crust, *Geol. Soc. Am. Mem.*, **132**, 195–205.
- Vine, F. J. & Wilson, J. T., 1965. Magnetic anomalies over a young oceanic ridge off Vancouver Island, *Science*, **150**, 485–489.
- Watkins, N. D. & Haggerty, S. E., 1967. Primary oxidation variation and petrogenesis in a single lava, *Contr. Mineral. Petrol.*, **15**, 251.
- Weissel, J. K. & Hayes, D. E., 1972. Magnetic anomalies in the southeast Indian Ocean, in *Antarctic oceanology II: the Australian–New Zealand sector*, ed. Hayes, D. E., AGU Antarctic Research Series, **19**, 165–196, Washington, DC.
- Williams, D. L., Von Herzen, R. P., Sclater, J. G. & Anderson, R. N., 1974. The Galapagos spreading centre: lithospheric cooling and hydrothermal circulation, *Geophys. J. R. astr. Soc.*, **38**, 587–608.
- Wilson, R. L. & Watkins, N. D., 1967. Correlation of petrology and natural remanent polarity in Columbia Plateau basalts, *Geophys. J. R. astr. Soc.*, **12**, 405–424.
- Wilson, R. L., Haggerty, S. E. & Watkins, N. D., 1968. Variation of palaeomagnetic stability and other parameters in a vertical traverse of a single Iceland lava, *Geophys. J. R. astr. Soc.*, **16**, 79.